Determining the Surface-To-Bulk Progression in the Normal-State Electronic Structure of Sr_2RuO_4 by Angle-Resolved Photoemission and Density Functional Theory

C. N. Veenstra,[1] Z.-H. Zhu,[1] B. Ludbrook,[1] M. Capsoni,[1] G. Levy,[1,2] A. Nicolaou,[1,2] J. A. Rosen,[1] R. Comin,[1] S. Kittaka,[3] Y. Maeno,[3] I. S. Elfimov,[1,2] and A. Damascelli[1,2,*]

[1]*Department of Physics & Astronomy, University of British Columbia, Vancouver, British Columbia V6T 1Z1, Canada*
[2]*Quantum Matter Institute, University of British Columbia, Vancouver, British Columbia V6T 1Z4, Canada*
[3]*Department of Physics, Graduate School of Science, Kyoto University, Kyoto 606-8502, Japan*

(Received 25 May 2012; published 1 March 2013)

We revisit the normal-state electronic structure of Sr_2RuO_4 by angle-resolved photoemission spectroscopy with improved data quality, as well as *ab initio* band structure calculations in the local-density approximation with the inclusion of spin-orbit coupling. We find that the current model of a single surface layer $(\sqrt{2} \times \sqrt{2})R45°$ reconstruction does not explain all detected features. The observed depth-dependent signal degradation, together with the close quantitative agreement with the slab calculations based on the surface crystal structure as determined by low-energy electron diffraction, reveal that—at a minimum—the subsurface layer also undergoes a similar although weaker reconstruction. This model accounts for all features—a key step in understanding the electronic structure—and indicates a surface-to-bulk progression of the electronic states driven by structural instabilities. Finally, we find no evidence for other phases stemming from either topological bulk properties or, alternatively, the interplay between spin-orbit coupling and the broken symmetry of the surface.

DOI: 10.1103/PhysRevLett.110.097004 PACS numbers: 74.25.Jb, 74.70.Ad, 79.60.Bm, 79.60.Jv

Since its discovery [1], understanding the origin of superconductivity in Sr_2RuO_4 has received enormous attention [2]. In search of the prodromes of the elusive pairing mechanism, its normal-state electronic structure has also been a matter of intense study. A unified picture of the Fermi surface (FS) was obtained from bulk-sensitive de Haas–van Alphen (dHvA) measurements [3,4] and surface sensitive angle-resolved photoemission spectroscopy (ARPES) [5]. This, together with local-density approximation (LDA) band structure calculations [6,7], established the importance of spin-orbit (SO) coupling in defining the low-energy electronic structure. The inclusion of SO coupling may also lie at the root of the bigger question regarding the superconducting mechanism, with suggestions that it may facilitate mixed-parity pairing [6,8,9].

Similar to the case of topological insulators the presence of SO coupling also raises the possibility that novel topological states, Dirac or Rashba-type, might exist on the (001) cleaving-surface of Sr_2RuO_4 in the normal state (in addition to the chiral superconductivity topological edge states detected below T_c on the side surfaces [10]). This proposal is particularly intriguing given that surface-specific electronic states have been observed in this material [5,11]. While these have originally been interpreted in terms of a purely structural reconstruction of the top surface layer [5,11] as resolved via low-energy electron diffraction (LEED) [12], a recent ARPES study detected an additional dispersive band [13]. This demands that this simple model be revisited in terms of a possible manifestation of topological bulk properties or, alternatively, Rashba interaction at the surface.

Here we study the normal-state electronic structure of Sr_2RuO_4 by ARPES and density-functional theory. With improved data quality a multitude of new dispersive features can be detected, stemming from the folding of *all* FSs: reconstructed-surface's and bulklike's as well. While this might be suggestive of surface ferromagnetism or Rashba-type splitting, we show—through controlled aging and LDA + SO slab calculations for the LEED-determined crystal structure [14]—that this doubling arises from surface and subsurface instabilities. This discovery bears close similarity to the recent findings of surface-enhanced charge-density-wave [15] and stripe [16] order in the underdoped high-T_c cuprates, establishing structural or electronic instabilities in the near surface region, a widespread phenomenon of complex oxides.

ARPES experiments were performed at UBC with a SPECS Phoibos 150 analyzer and 21.2 eV photons from a monochromatized UVS300 lamp. FWHM energy and momentum resolutions were measured to be 17 meV and 0.01 π/a angular equivalent in Figs. 1 and 2 and 9 meV and 0.04 $\pi/\sqrt{2}a$ in Fig. 3. Samples grown by the floating-zone method [17] were oriented by Laue diffraction, cleaved *in situ*, then held at temperatures between 5–10 K and pressures varied in the $5–9 \times 10^{-11}$ mbar range. To verify that the observed ARPES features are not associated with Ru-metal inclusions, the so-called "3 K phase" [17], samples with and without inclusions were studied: no 3 K-phase dependence was observed in these features.

Let us begin with a brief review of the previously accepted electronic structure from bulk and reconstructed surface [5,6,11]. Figure 1(a) shows the LDA + SO bulk FS

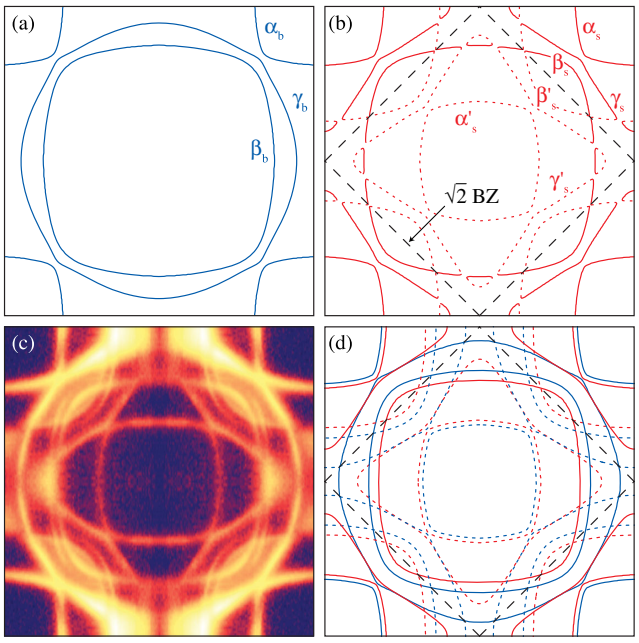

FIG. 1 (color online). The LDA + SO, $k_z = 0$ FS of Sr_2RuO_4 for: (a) undistorted bulk; (b) bulk with RuO_6 octahedra rotated 5.5° causing a $(\sqrt{2} \times \sqrt{2})R45°$ reconstruction (new BZ, dashed line; unfolded FS, solid line; folded replica FS, dotted line). (c) ARPES FS (7 meV integration) from a fresh low-temperature cleave; (d) phenomenological FS based on (c), Figs. 2 and 3.

derived from the Ru-t_{2g} orbitals occupied by four electrons, which is in good agreement with results from dHvA [3,4], as well as ARPES on an optimally degraded surface [5]. As a consequence of the $(\sqrt{2} \times \sqrt{2})R45°$ surface reconstruction observed by LEED [12] and associated with the rotation of the RuO_6 octahedra [Fig. 4(c)], the Brillouin Zone (BZ) is reduced leading to band folding; this is shown in Fig. 1(b) for a 5.5°-rotation LDA + SO bulk calculation (note that primes and dotted lines will be used for folded FSs, and s (red) for surface and b (blue) for bulklike states). In Fig. 1(c) we present the ARPES FS for a pristine cleave of Sr_2RuO_4, measured in p polarization at 5 K and 6×10^{-11} mbar in less than 3 hours after cleaving, during which time no aging was observed. The data were acquired over the entire upper right quadrant without symmetrization, then folded in k space to reproduce the BZ as shown (the analyzer entrance slit was oriented horizontally with respect to the final image, giving greater angular resolution in that direction). One can recognize doubling and folding of many features, seemingly consistent with the overlap of bulk and reconstructed FSs from Figs. 1(a) and 1(b), as originally proposed [5,11]. For instance, both β_b and β_s are seen, as well as both γ_b and γ_s with their expected electron and holelike topology [with γ_s showing clearly near $(0, \pi)$ and γ_b near $(\pi, 0)$, due to varying matrix element dependence]. However, contrary to this explanation, the folded β' also is clearly doubled giving rise to β'_b and β'_s. We will show in Figs. 2 and 3 that in fact *all* bands are doubled—both unfolded *and folded*—resulting in the phenomenological FS of Fig. 1(d). This cannot be explained by a single reconstructed surface-layer model, and may instead be consistent with the interesting proposal of SO-driven surface effects [13].

In Fig. 2 we confirm the doubling of features with momentum distribution curves (MDCs) obtained by integrating a 10 meV region just above E_F: panels (b)–(e) show the doubling of β, β', α, and α', respectively, observed at the k locations indicated in the alignment FS of (a). Note that the splitting between α'_s and α'_b is more clearly resolved in the second BZ [Fig. 2(e)], perhaps due to matrix element effects and/or second-BZ higher angular resolution. By performing a least-squares fit to two Lorentzian peaks with a second-order polynomial background (black curves), we can estimate the observed splittings as: 0.057, 0.065, 0.027, and $0.029 \pm 0.003\ \pi/a$ for β, β', α, and α'. Although it is difficult to compare these values directly, due to the slight difference in angles and k-space locations between them, we note that the splittings between β_s/β_b and β'_s/β'_b are very close and approximately double those between α_s/α_b and α'_s/α'_b, which are almost identical.

Thus far, with a doubling observed for all α and β bands and in light of the bulk magnetism of many Ru oxides, one might be drawn to the possibility of Rashba-type effects

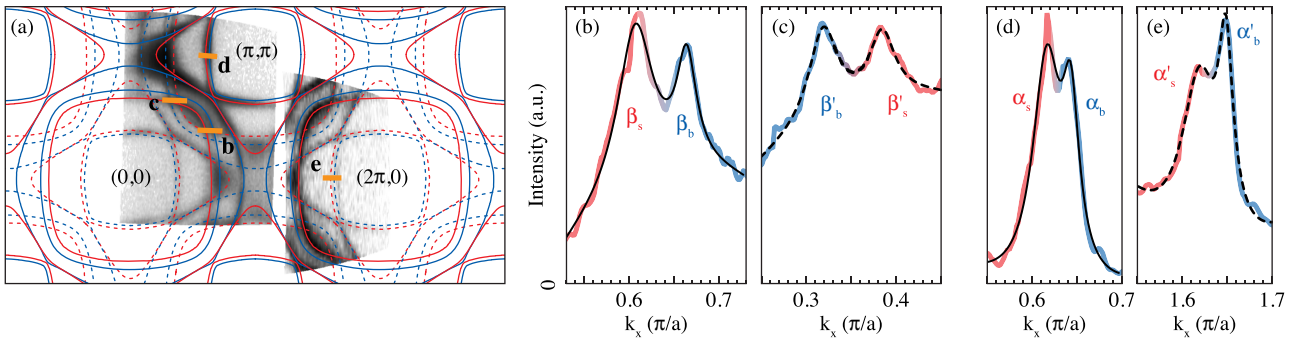

FIG. 2 (color online). (a) Sr_2RuO_4 FS maps (grey scale), marking the location of MDC cuts at the Fermi energy showing clear doubling in the (b) β sheet, (c) its folded replica β', (d) α, and (e) folded α'. (b)–(e) Data are shown in color, with red and blue referring to surface and bulklike features, while fit results (see text) are shown in black (dashed lines for folded bands).

[13] or even surface ferromagnetism [12]. If any of these were the case one would expect that—under surface degradation—the surface states' splitting would shrink and/or the intensity decay uniformly over time for all of them, eventually revealing the underlying bulk electronic structure. In Fig. 3 we show the results of such a time-dependent experiment for the band dispersion along the $(0,0) - (\pi,\pi)$ direction in s polarization, where all features and their folded replicas are visible simultaneously, for a sample maintained at 9.5 K while raising the base pressure to about 8.5×10^{-11} mbar.

The time evolution of MDCs integrated over 100 minutes and 4 meV just above E_F is presented in Fig. 3(a): while some features remain at a similar level of intensity over the 14-hour time span, others age and have their intensity suppressed, without any overall change in slope or shape. Particularly comparing Fig. 3(c) with 3(d), 3(e) with 3(f), and 3(g) with 3(h), which present only first and final MDC and dispersion results, we can infer that (i) *all* bands and their folded replicas are doubled for a total of 12 bands (as labelled), including the γ bands not previously demonstrated in Fig. 2, and (ii) based on the observed difference in degradation rate, the electronic states do not all originate from the very same surface layer, and can instead be classified as surface (fast degradation) or bulklike (slow degradation). These observations can be made more quantitative from the MDC-dispersion fit analysis, which allows distinguishing between surface and bulklike bands based on their remarkably different Fermi velocity v_F (see Table I). While the fresh data in Fig. 3(g) are dominated by the surface α_s/α'_s, β_s/β'_s, and γ_s/γ'_s, with the addition of the well-separated β_b/β'_b pair, the aged data of Fig. 3(h) only show the much steeper bulklike α_b/α'_b, β_b/β'_b, and γ_b/γ'_b (α'_b, although visible, could not be fit and is shown with a dashed line as a guide to the eye).

Since all s states are suppressed evenly and independently from the b ones, we must conclude that neither ferromagnetism nor Rashba coupling is responsible for the apparent band doubling. Similarly, we must rule out possible surface patches with different structure or effective doping, as well as bulk photoelectrons being scattered off the reconstructed surface [18]. As intrinsic bulk properties can also be excluded, otherwise they would be visible in dHvA [3,4] and x-ray diffraction [24], the most natural explanation would be that the subsurface layer has a structural modulation similar to, yet weaker, than that found at the surface. This lesser modulation would be enough to break the symmetry of the BZ and cause a visible folding, but not enough to strongly modify FS topologies and volumes. The subsurface layer is then responsible for all b states while the surface for s states. Measured FS volumes [Figs. 1(c) and 1(d)] support this model: as shown in Table I, while the s-FS electron counting is somewhat reduced ($n_e^s \simeq 3.87$), the b-FS electron counting is much closer to the dHvA results adding up to

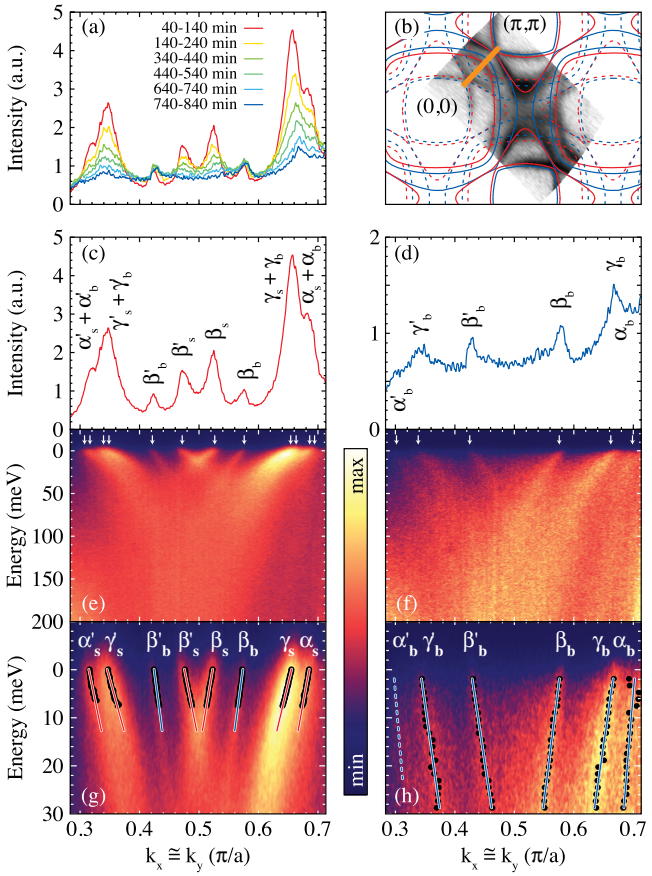

FIG. 3 (color online). (a) Time evolution of a 45° MDC cut at E_F; its location is marked on the alignment FS in (b). (c), (e), (g) Plot of the corresponding MDC at E_F, band map of features on a large energy range, and zoom in energy on the Fermi crossings for the first 100 minutes after cleave; (d), (f), (h) the same for the final 100 minutes of acquisition. In (g), (h), MDC maxima (black circles) and MDC-dispersion fits (blue—bulk and red—surface lines) are also shown.

$n_e^b \simeq 3.94$, i.e., almost four electrons as expected in the Ru t_{2g} orbitals (this still seems to suggest the possibility that these near-surface layers are slightly hole doped, possibly due to the cleaving-induced Sr vacancies revealed by scanning tunnelling microscopy [25]). Finally photoemission from a second layer, also folded but otherwise similar to the bulk, could even explain the so-called "shadow band" which remained after high-temperature cleaving had suppressed the surface states in the original work uniting the dHvA and ARPES pictures of the FS of Sr_2RuO_4 [5].

To conclusively validate this explanation we have performed a 5-RuO_2-layer LDA + SO slab calculation using the linearized augmented-plane-wave method in the WIEN2K package [26,27]. Explicitly including these layers and the vacuum in the unit cell allows us to study both the structural reconstruction as well as effects due to broken symmetry in proximity of the surface in a self-consistent way. Additionally, this enables us to estimate the surface or bulk character of the resulting bands by projecting the

TABLE I. Carrier concentrations counting electrons, $n_e = 2 \times A_{FS}/A_{BZ}$ with 2 accounting for the spin degeneracy, and Fermi velocities along the $(0,0) - (\pi,\pi)$ direction, v_F, as determined by our ARPES and LDA + SO slab calculations for surface and bulklike electronic structure. ARPES-FS volume estimates are from the phenomenological FS in Fig. 1; LDA + SO results were obtained for the 24 meV shifted chemical potential to match the average electron counting of surface and subsurface FSs as determined by ARPES. The dHvA results from Ref. [4], representative of the bulk Luttinger's counting, are also shown.

Band	$n_e^{\mathrm{LDA+SO}}$	$v_F^{\mathrm{LDA+SO}}$ (eV Å)	n_e^{ARPES}	v_F^{ARPES} (eV Å)	$v_F^{\mathrm{LDA+SO}}/v_F^{\mathrm{ARPES}}$	n_e^{dHvA}
α_s, α_s'	1.668 ± 0.007	2.30 ± 0.01	1.721 ± 0.040	0.56 ± 0.05	4.1 ± 0.4	···
β_s, β_s'	0.864 ± 0.006	2.14 ± 0.01	0.757 ± 0.020	0.59 ± 0.05	3.6 ± 0.3	···
γ_s, γ_s'	1.340 ± 0.011	2.18 ± 0.02	1.396 ± 0.060	0.42 ± 0.05	5.2 ± 0.6	···
Total	3.872 ± 0.014	···	3.874 ± 0.120	···	···	···
α_b, α_b'	1.740 ± 0.003	2.14 ± 0.02	1.760 ± 0.040	1.30 ± 0.60	1.6 ± 0.8	1.781
β_b, β_b'	0.967 ± 0.022	2.60 ± 0.25	0.903 ± 0.020	0.80 ± 0.10	3.3 ± 0.5	0.921
γ_b, γ_b'	1.252 ± 0.014	2.21 ± 0.07	1.280 ± 0.060	0.76 ± 0.10	2.9 ± 0.4	1.346
Total	3.959 ± 0.026	···	3.943 ± 0.120	···	···	4.048

corresponding wave functions onto the Ru orbitals for each layer. We used a symmetric slab with two surface layers surrounding three bulklike layers [Figs. 4(a) and 4(b)], and the surface structure as determined by LEED [14]. This consists of a 7.46° rotation and a ∼1% elongation of the surface RuO_2 octahedra, as well as slightly modified surface Sr positions. The resulting constant energy contour at 24 meV binding energy, corresponding to a FS with an averaged electron counting $n_e \simeq 3.91$ to match the *s-b* averaged value experimentally observed by ARPES, is shown in Fig. 4(c): two sets of red FSs pertaining to the two outer surface layers, and three blue FS sets for the three bulk layers; hybridization between layers does occur at some *k* points, where sheets can be seen to change character.

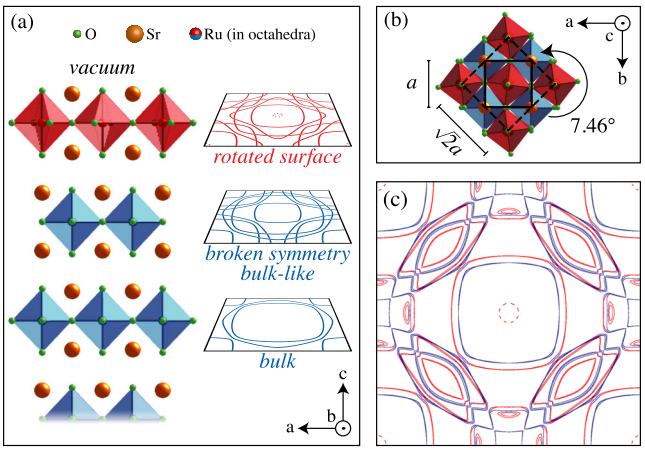

FIG. 4 (color online). (a) Partial structure of the Sr_2RuO_4 five-layer slab used for LDA + SO calculations, with corresponding surface and bulklike FS. (b) Reconstructed surface of Sr_2RuO_4, with the original undistorted unit cell shown solid and new shown dashed. (c) FS obtained from the LDA + SO slab calculations by shifting the chemical potential 24 meV down in energy to match the slight averaged hole doping observed by ARPES for Sr_2RuO_4 surface and bulklike FS. Surface and bulk character are shown in red and blue, respectively.

Although somewhat complicated by hybridization gaps appearing at all crossings, and a δ_s pocket of $d_{x^2-y^2}$ character at (0,0) and (π,π) which experimentally is found just above E_F [11], these calculations show good overall agreement with the phenomenological FS concerning the splitting, topology, and volume of the various bands (Table I); as well as—and most importantly—the surface versus bulklike assignment of all detected features.

To conclude, by means of ARPES and LDA + SO slab calculations we have been able to unravel the surface-to-bulk progression of the electronic structure in Sr_2RuO_4. We find that a $(\sqrt{2} \times \sqrt{2})R45°$ reconstruction of surface and subsurface layers provides a consistent explanation of all detected dispersive features in terms of a progression of electronic states induced by structural instabilities, with no evidence for novel phases driven by topological bulk properties, ferromagnetic ordering, or the interplay between SO coupling and the broken symmetry of the surface. This layer-by-layer approach provides the most detailed information on FS volumes, Fermi velocities, as well as many body renormalizations $v_F^{\mathrm{ARPES}}/v_F^{\mathrm{LDA+SO}}$, for both surface and bulklike bands (Table I). In analogy with the recent work on underdoped cuprates [15,16], which found evidence for the enhancement of electronic correlations and ordering tendencies in the surface and subsurface region, our study of Sr_2RuO_4 also highlights the significantly more correlated character of the top surface layer bands, which might thus more strongly benefit from a LDA + SO + U description [7]. As a matter of fact, the inclusion of $U =$ 1 eV (not shown) immediately leads to the lifting of the δ_s FS predicted by LDA + SO, as a result of the overall *U*-driven bandwidth renormalization.

We acknowledge C. Bergemann, M. W. Haverkort, R. G. Moore, and G. A. Sawatzky for discussions; D. Wong and P. Dosanjh for technical assistance. This work was supported by the Max Planck—UBC Centre for Quantum Materials (A. N.), CRC and NSERC's Steacie Memorial Fellowship Programs (A. D.), NSERC, CFI, CIFAR Quantum Materials, and MEXT KAKENHI (No. 22103002).

*damascelli@physics.ubc.ca

[1] Y. Maeno, H. Hashimoto, K. Yoshida, S. Nishizaki, T. Fujita, J. G. Bednorz, and F. Lichtenberg, Nature (London) **372**, 532 (1994).

[2] Y. Maeno, S. Kittaka, T. Nomura, S. Yonezawa, and K. Ishida, J. Phys. Soc. Jpn. **81**, 011009 (2012).

[3] A. P. Mackenzie, S. R. Julian, A. J. Diver, G. J. McMullan, M. P. Ray, G. G. Lonzarich, Y. Maeno, S. Nishizaki, and T. Fujita, Phys. Rev. Lett. **76**, 3786 (1996).

[4] C. Bergemann, S. R. Julian, A. P. Mackenzie, S. NishiZaki, and Y. Maeno, Phys. Rev. Lett. **84**, 2662 (2000).

[5] A. Damascelli, D. H. Lu, K. M. Shen, N. P. Armitage, F. Ronning, D. L. Feng, C. Kim, Z.-X. Shen, T. Kimura, Y. Tokura, Z. Q. Mao, and Y. Maeno, Phys. Rev. Lett. **85**, 5194 (2000).

[6] M. W. Haverkort, I. S. Elfimov, L. H. Tjeng, G. A. Sawatzky, and A. Damascelli, Phys. Rev. Lett. **101**, 026406 (2008).

[7] G.-Q. Liu, V. N. Antonov, O. Jepsen, and O. K. Andersen, Phys. Rev. Lett. **101**, 026408 (2008).

[8] J. J. Deisz and T. E. Kidd, Phys. Rev. Lett. **107**, 277003 (2011).

[9] C. M. Puetter and H.-Y. Kee, Europhys. Lett. **98**, 27 010 (2012).

[10] S. Kashiwaya, H. Kashiwaya, H. Kambara, T. Furuta, H. Yaguchi, Y. Tanaka, and Y. Maeno, Phys. Rev. Lett. **107**, 077003 (2011).

[11] K. M. Shen, A. Damascelli, D. H. Lu, N. P. Armitage, F. Ronning, D. L. Feng, C. Kim, Z.-X. Shen, D. J. Singh, I. I. Mazin, S. Nakatsuji, Z. Q. Mao, Y. Maeno, T. Kimura, and Y. Tokura, Phys. Rev. B **64**, 180502 (2001).

[12] R. Matzdorf, Z. Fang, Ismail, J. Zhang, T. Kimura, Y. Tokura, K. Terakura, and E. W. Plummer, Science **289**, 746 (2000).

[13] V. B. Zabolotnyy, E. Carleschi, T. K. Kim, A. A. Kordyuk, J. Trinckauf, J. Geck, D. Evtushinsky, B. P. Doyle, R. Fittipaldi, M. Cuoco, A. Vecchione, B. Bchner, and S. V. Borisenko, New J. Phys. **14**, 063039 (2012).

[14] R. G. Moore, Ph.D. thesis, The University of Tennessee, 2006.

[15] J. A. Rosen, R. Comin, G. Levy, D. Fournier, Z.-H. Zhu, B. Ludbrook, C. N. Veenstra, D. Wong, P. Dosanjh, Y. Yoshida, H. Eisaki, L. Petaccia, and A. Damascelli, arXiv:1111.2673.

[16] H.-H. Wu, M. Buchholz, C. Trabant, C. Chang, A. Komarek, F. Heigl, M. Zimmermann, M. Cwik, F. Nakamura, M. Braden, and C. Schler-Langeheine, Nat. Commun. **3**, 1023 (2012).

[17] T. Ando, T. Akima, Y. Mori, and Y. Maeno, J. Phys. Soc. Jpn. **68**, 1651 (1999).

[18] In analogy with previous work on Bi cuprates, one may wonder if the subsurface folded bands detected in Sr_2RuO_4 might originate from the diffraction of bulk photoelectrons traveling through the reconstructed topmost surface layer. While the results of surface degradation are strong evidence against this, it is nevertheless important to explore the parallel with the Bi cuprates. There, two sets of unexpected features are detected in addition to the single band of the ideal CuO_2 square plane [19]: these have been referred to in the literature as ''shadow bands'' and ''umklapp bands'' [20]. It is the umklapp bands which were initially suspected to be due to the diffraction of the CuO_2 plane photoelectrons traveling through the modulated BiO surface layer, since they appeared to exhibit multiple positive and negative high-order replicas, consistent with a diffraction scenario. However, this was later shown not to be the case: all crystal planes present the same incommensurate modulations as the BiO planes, and the umklapp bands therefore stem from initial states *intrinsic* to the modulated CuO_2 plane and not from *extrinsic* photoelectron diffraction [15,21–23]. Additionally, it is not with the umklapp but with the shadow bands that the subsurface folded bands in Sr_2RuO_4 share their form of reconstruction. Importantly, contrary to the umklapp bands, these shadow bands in Bi cuprates were deemed inconsistent with a photoelectron diffraction scenario; by analogy, the same would hold for Sr_2RuO_4. While initially attributed to antiferromagnetic fluctuations giving rise to a $(\sqrt{2} \times \sqrt{2})R45°$ larger unit cell and a correspondingly folded Brillouin zone [19], the shadow bands in Bi cuprates were conclusively shown to arise from the presence of two structurally inequivalent Cu atoms per orthorhombic unit cell [15,21–23].

[19] P. Aebi, J. Osterwalder, P. Schwaller, L. Schlapbach, M. Shimoda, T. Mochiku, and K. Kadowaki, Phys. Rev. Lett. **72**, 2757 (1994).

[20] A. Damascelli, Z. Hussain, and Z.-X. Shen, Rev. Mod. Phys. **75**, 473 (2003).

[21] A. Mans, I. Santoso, Y. Huang, W. K. Siu, S. Tavaddod, V. Arpiainen, M. Lindroos, H. Berger, V. N. Strocov, M. Shi, L. Patthey, and M. S. Golden, Phys. Rev. Lett. **96**, 107007 (2006).

[22] K. Nakayama, T. Sato, T. Dobashi, K. Terashima, S. Souma, H. Matsui, T. Takahashi, J. C. Campuzano, K. Kudo, T. Sasaki, N. Kobayashi, T. Kondo, T. Takeuchi, K. Kadowaki, M. Kofu, and K. Hirota, Phys. Rev. B **74**, 054505 (2006).

[23] P. D. C. King, J. A. Rosen, W. Meevasana, A. Tamai, E. Rozbicki, R. Comin, G. Levy, D. Fournier, Y. Yoshida, H. Eisaki, K. M. Shen, N. J. C. Ingle, A. Damascelli, and F. Baumberger, Phys. Rev. Lett. **106**, 127005 (2011).

[24] L. Walz and F. Lichtenberg, Acta Crystallogr. Sect. C **49**, 1268 (1993).

[25] Y. Pennec, N. J. C. Ingle, I. S. Elfimov, E. Varene, A. Damascelli, J. V. Barth, and Y. Maeno, Phys. Rev. Lett. **101**, 216103 (2008).

[26] P. Blaha, K. Schwarz, G. K. H. Madsen, D. Kvasnicka, and J. Luitz, in *An Augmented Plane Wave Plus Local Orbitals Program for Calculating Crystal Roperties*, edited by K. Schwarz (Technical University of Wien, Vienna, 2001).

[27] See Supplemental Material at http://link.aps.org/supplemental/10.1103/PhysRevLett.110.097004 for additional details about the slab calculations.

Auxiliary Material for:

Determining the Surface-To-Bulk Progression in the Normal-State Electronic Structure of Sr_2RuO_4 by Angle-Resolved Photoemission and Density Functional Theory

C. N. Veenstra, Z.-H. Zhu, B. Ludbrook, M. Capsoni, G. Levy, A. Nicolaou, J. A. Rosen, R. Comin, S. Kittaka, Y. Maeno, I. S. Elfimov, A. Damascelli

Crystal structure used in the LDA+SO slab calculations

In order to determine the structure to use for slab calculations, bulk band structure calculations in the local density approximation with spin-orbit coupling (LDA+SO) were performed for crystal structures where the Ru oxygen octahedra were modified to have a variety of different rotations (with unit cell dimensions kept constant). This allowed the exploration of a larger parameter space without the computational expense of multiple slab calculations. In Fig. S1(a) we see that, for rotations under $\sim 3^\circ$, no significant change in Fermi surface volume (average 3%) is observed, with in particular no change in the topology of the γ Fermi surface [correspondingly the γ band Van Hove singularity at the M point remains above the Fermi level in Fig.S1(b)]. For rotations above $\sim 5.5^\circ$ the topology of the γ band changes to match that of the surface, and $\sim 7.5^\circ$ introduces also the δ band at Γ/X. Comparing these calculations to experiments then suggests that any subsurface rotation should be $\lesssim 3^\circ$ while the surface rotation should be $\gtrsim 5^\circ$ (keeping in mind that the δ crossing moves above the Fermi level with the inclusion of U, so $\sim 7.5^\circ$ is not a hard upper limit).

The exact slab structure chosen for the LDA+SO slab calculations is presented in detail in Fig. S2. This includes a surface layer chosen to match that measured by LEED, whose 7.46° rotation compares well with that expected from the above bulk calculations. However, the exact nature of the subsurface layer is unknown and cannot be probed accurately. Since the choice of any finite small rotation in the subsurface layer would be largely arbitrary, and unnecessary in order to simply introduce a folding due to the nature of the calculations, we chose to use a pure bulk-like structure for the inner 3 layers as the simplest possible model. This also allowed the realization – with only 5 layers – of a bulk-like region with large size compared to the surface-like region.

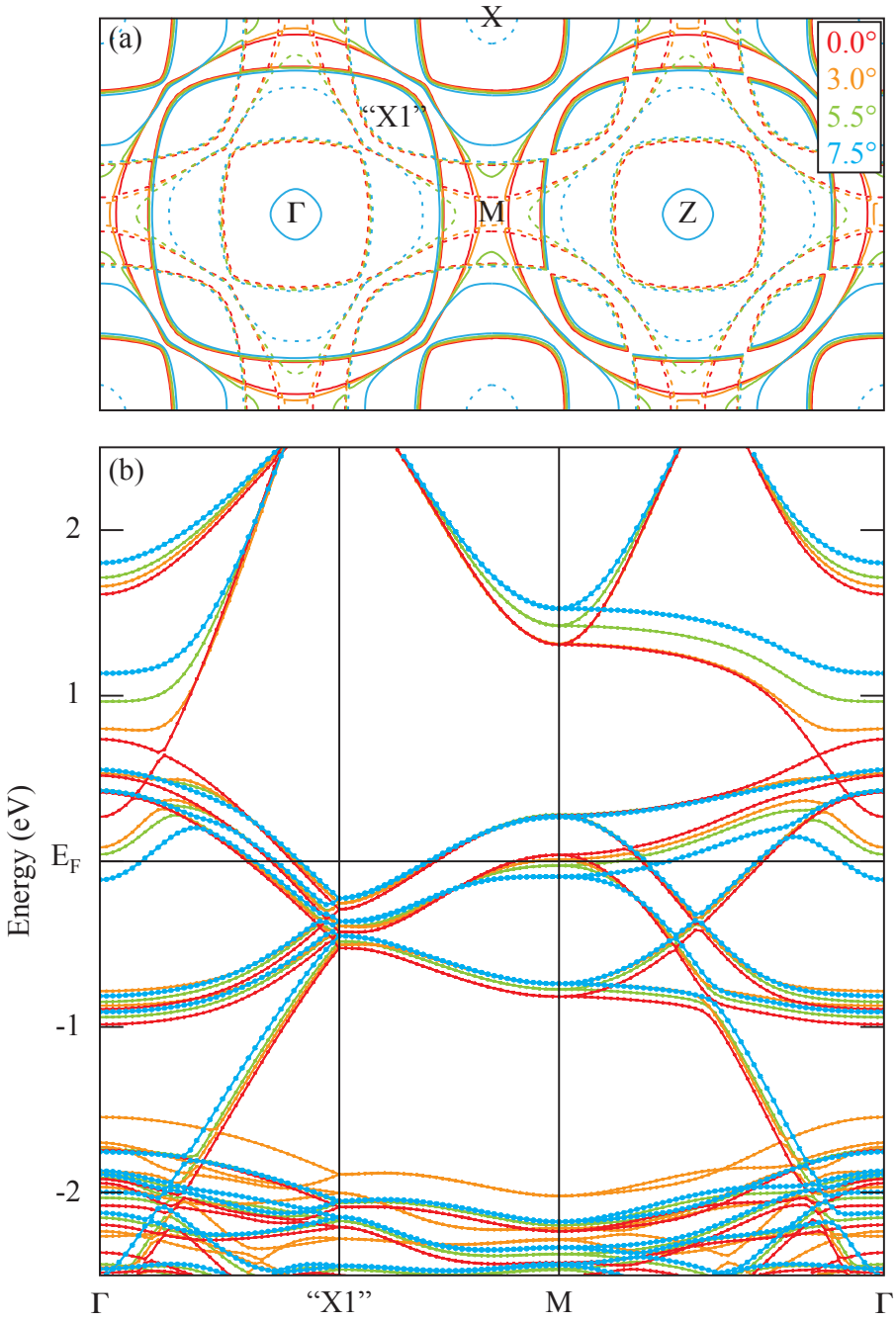

Figure S1: (color online). (a) Fermi surface and (b) band structure from bulk LDA+SO calculations for incremental rotations of the oxygen octahedra.

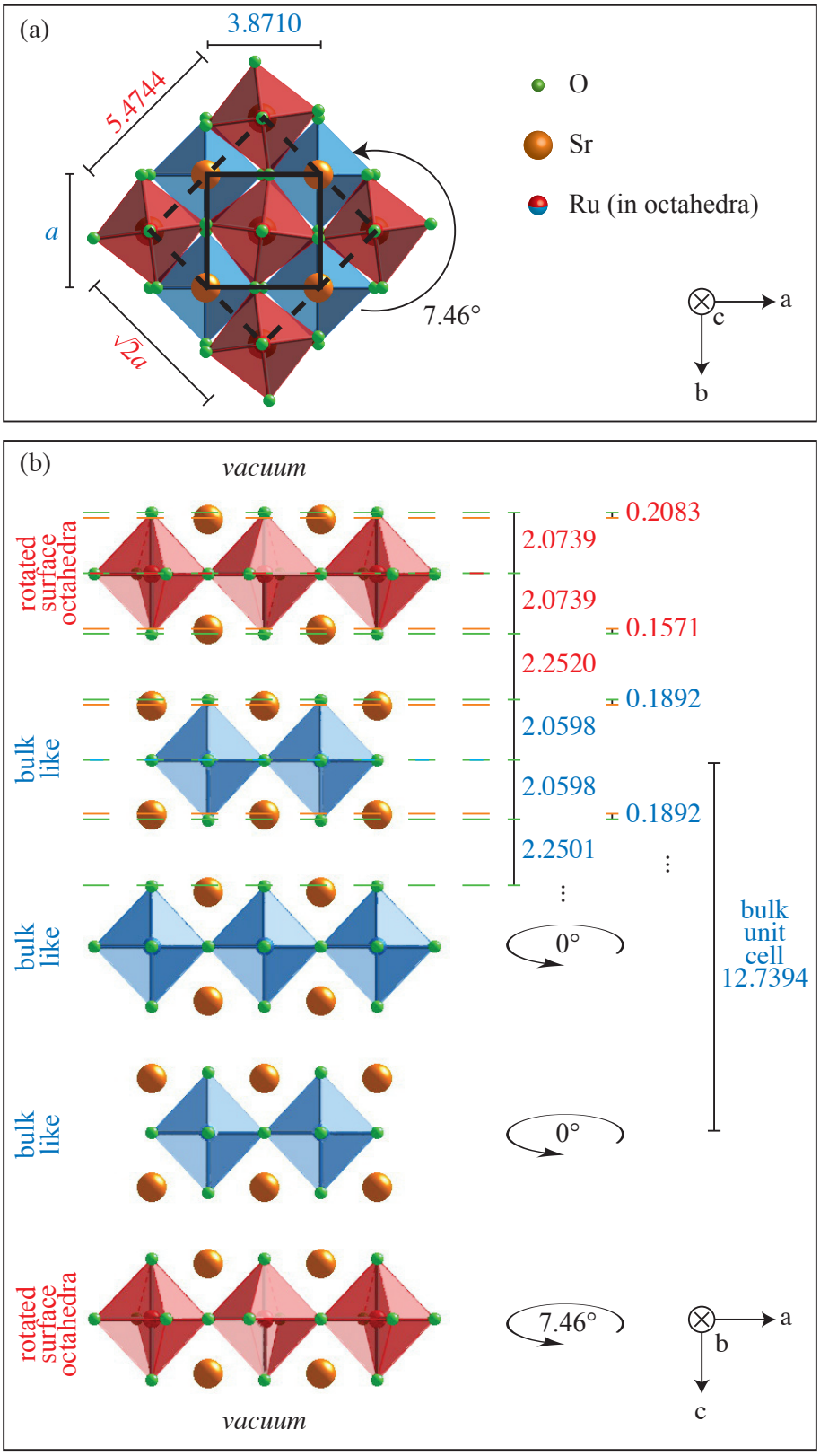

Figure S2: (color online). Atomic positions in the 5 layer slab used for LDA+SO calculations, viewed from (a) above and (b) the side. All dimensions are in Å.